

Spectroscopic Study of DNA Hydrolysis, DNA Intercalative, and Electrostatic Interaction Activity Exerted by Drug Based Coordination Compounds

Mohan N. Patel,^{*,[a]} Bhupesh S. Bhatt,^[a] and Promise A. Dosi^[a]

Keywords: Hydrolytic cleavage; DNA cleavage; DNA degradation; Bactericidal activity; Copper

Abstract. Our work emphasized on synthesizing and characterizing neutral mononuclear copper(II) complexes with second generation fluoroquinolone drug ciprofloxacin (CFL) and some bipyridine derivatives (A'') of type $[Cu(CFL)(A'')Cl] \cdot 2H_2O$. The DNA binding free energies were evaluated by studying the effect of salt concentrations on DNA binding. DNA interactions were investigated by using DNA melting temperature studies, viscosity measurements, absorption ti-

tration, and gel electrophoresis experiments. Also superoxide dismutase (SOD)-like activity (IC_{50} values) and antibacterial activity of metal complexes were studied. To validate the proper mechanistic pathway for plasmid DNA cleavage, gel electrophoresis experiments were carried out in presence of radical scavenging agents. The bactericidal activity of metal complexes was evaluated in terms of colony forming unit.

Introduction

DNA-interacting molecules are of importance in medicine and the understanding of their interaction with specific sequences is the fundamental key in any attempt to control gene expression through drug binding.^[1–3] Deoxyribonucleic acid (DNA) is the primary target molecule for most anticancer and antiviral therapies according to cell biology.^[4] Transition metal complexes can interact non-covalently with DNA in various binding modes e.g. intercalation, groove binding, and external electrostatic binding. Investigations of the interactions of DNA with transition metal complexes are performed to design new types of the pharmaceutical molecules, to elucidate the mechanisms involved in the site specific recognition of DNA and to determine the principles governing the recognition.^[5]

Metal ions are often classed as toxic or non-toxic, however their biological activity depends very much on speciation and it is now widely accepted that, with carefully controlled coordination chemistry, even toxic metals can exhibit therapeutic properties.^[6] Among all the mechanism of detoxification, chelation by various ligands or proteins like metallothioneins or phytochelatins provides greater resistance to the toxic effects of the heavy metals.^[7] Metal ions and coordination compounds are known to affect the cellular processes dramatically,^[8] not only by affecting the natural processes like cell division, gene expression, etc., but also by some non-natural processes like

toxicity, carcinogenicity, anti-tumor, etc. Copper is found in a variety of enzymes, including the copper atoms of cytochrome-c oxidase and the enzyme superoxide dismutase (SOD, containing copper and zinc), and is the central metal ion in the oxygen-carrying pigment hemocyanin. In accumulation to its enzymatic roles, copper is used for biological electron transport. Due to extensive bioavailability and less toxicity of copper in comparison with other metal ions, it is the metal of choice for the latest research in bioinorganic and medicinal chemistry. Since the discovery of bis(phen)copper(I) complex as the first copper-based “chemical nuclease”,^[9] many attempts have been made to study copper(II) complexes of phenanthrolines/bipyridines/bipyridylamines in combination with the quinolone family drugs nalidixic acid,^[10] cinoxacin,^[11] ciprofloxacin,^[12] *N*-propyl-norfloxacin,^[13] ofloxacin,^[14] as antitumor, antibacterial, antimicrobial,^[15] DNA intercalating,^[16] artificial nucleases,^[17] and SOD mimic agents.^[18] Copper can be extremely useful in mounting the new agents that can serve mankind by their action against severe diseases.

Ciprofloxacin, the second generation fluoroquinolone drug, is a broad-spectrum antibiotic that is active against Gram(+ve) and Gram(-ve) microorganisms. It functions by suppressing cell growth by inhibiting one step of the multi-step activity of the enzyme DNA gyrase, which can introduce super-coils into closed-circular DNA using the free energy of ATP hydrolysis. Quinolone-induced DNA damage was first reported in 1986.^[19–21] Ciprofloxacin has 12 FDA approved human uses and other veterinary uses. Since the evolving problem of drug resistance to microorganisms, the latest researches are going on finding applicability of coordination effect to enhance the biological potency of ligands or drug molecules.^[22,23]

The thermodynamic profile of DNA binding is needed for the proper understanding of interactions between DNA and

* Prof. Dr. M. N. Patel
E-Mail: jeenen@gmail.com

[a] Department of Chemistry
Sardar Patel University,
Vallabh Vidyanagar
388120 Gujarat, India

Supporting information for this article is available on the WWW under <http://dx.doi.org/10.1002/zaac.201100307> or from the author.

binding moieties. Our experimental studies provide data of general interest and use in addressing the larger issues concerned with developing appropriate thermodynamic descriptions of DNA binding free energy. Researching DNA binding model of the fluoroquinolones and their transition metal complexes can bring many innovations in the antitumor, antiviral, antibacterial, and antiaging fields of medicine. In continuation to our earlier work,^[24] in this paper, mixed ligand complexes of Cu^{II} with ciprofloxacin and neutral N,N-donor bidentate ligands were synthesized in order to evaluate their DNA binding properties. Bactericidal activity against Gram(+ve) and Gram(-ve) bacteria were assayed in terms of colony forming unit.

Results and Discussion

Characterization of Metal Complexes

The elemental analysis is in good concurrence with the proposed 1:1:1, metal:CFL:Aⁿ formulation.

IR Spectroscopy

Ring mode vibrations of the ligands are affected by coordination to Cu^{II}, corresponding to shift in energy for bands in the 1700–500 cm⁻¹ region of IR spectra. In the IR spectra of complexes, these bands are also slightly sensitive to the substituent of ligands. The prominent IR spectroscopic data of the complexes are shown in Table 1. The broad band in quinolone at approx. 3010 cm⁻¹ is due to hydrogen bonding, which contributes to ionic resonance structure and the observed peak was of free hydroxyl stretching vibration. The complete elimination of this broad band can be ascribed to presence of covalent bond between copper and -COO⁻ of ciprofloxacin. The $\nu(\text{C}=\text{O})$ stretching vibration band appears at 1708 cm⁻¹ for ciprofloxacin, whereas for the complexes it appears at 1619–1627 cm⁻¹. This shift towards lower energy suggests that coordination occurs through the carbonyl oxygen of pyridine ring.^[25] The strong absorption bands at 1624 cm⁻¹ and 1340 cm⁻¹ in ciprofloxacin could be assigned for $\nu(\text{COO})$ asymmetric and symmetric vibrations respectively, whereas in the metal complexes, these bands are observed at 1561–1581 and 1355–1378 cm⁻¹. The difference $\Delta = \nu_{\text{asym}}(\text{CO}_2) - \nu_{\text{sym}}(\text{CO}_2)$ is very much informative in determining the coordination mode of the ligands. If the difference is greater than 200 cm⁻¹, it would point towards monodentate coordination

behavior of the carboxylato group^[26–28] of ciprofloxacin. These data are further supported by $\nu(\text{M}-\text{O})$ bands,^[29] which appear at 509–520 cm⁻¹ for complexes.

The $\nu(\text{C}=\text{N})$ band of bipyridine derivatives is usually observed at about 1414 cm⁻¹. It is shifted to higher frequency at approx. 1459 cm⁻¹ in the complexes, which suggests the bidentate N–N coordination of the ligand.^[26,30,31] The $\nu(\text{M}-\text{N})$ band at 532–544 cm⁻¹ is assigned to N→M bonding of complexes.^[26,32] So the IR spectroscopic study suggests coordination of ciprofloxacin from pyridone oxygen and carboxylic hydroxyl group, whereas coordination of bipyridines occurs through two nitrogen atoms.

FAB-Mass Spectrometry

Figure 1 represents the FAB-mass spectrum of complex [Cu(CFL)(A¹)Cl]·2H₂O (**1**) obtained using *m*-nitro benzyl alcohol as matrix. Peaks at 136, 137, 154, 289, and 307 *m/z* value are due to usage of matrix. The molecular ion peak is observed at *m/z* = 772. The M+2 peak at 774 *m/z* value with 1/3 intensity to molecular ion peak demonstrate Cl⁻ ion attachment with metal ion. Furthermore, the peak at 737 *m/z* can be ascribed for removal of covalently bonded Cl⁻ ion. The most intense peak was observed at *m/z* = 342. Figure 1 shows peaks at 737, 442, 405, 342, and 330 *m/z* values. The *m/z* values correspond to peaks for particular fragments are duly highlighted in fragmentation pattern of complex **1** (Figure S1, Supporting Information)).

Reflectance Spectroscopy and Magnetic Behavior

Complexes of copper(II) with different coordination numbers result in different arrangements. The electronic absorption bands of copper(II) complexes resulting from the d–d transitions are referred as ligand field or crystal field bands because their energies shift correspond to the positions of ligands in the spectrochemical series. The copper(II) complexes exhibit broad bands at ambient temperature in the region 16000–18000 cm⁻¹. These bands are characteristic of Cu^{II} d–d transition in tetragonal field, in which the Cu^{II} atom is in a distorted square-pyramidal coordination environment,^[10,33] which is the only possible arrangement for the metal complexes.

The magnetic moments measurement for any arrangement in copper(II) complexes generally results in 1.8 BM, which is very close to spin-only value i.e. 1.73 BM. The observed val-

Table 1. Characteristic absorptions bands /cm⁻¹ of IR spectra of complexes **1–8** and CFLH.

	$\nu(\text{C}=\text{O})$ pyridone	$\nu(\text{COO})_{\text{asy}}$	$\nu(\text{COO})_{\text{sy}}$	$\Delta\nu$	$\nu(\text{M}-\text{N})$	$\nu(\text{M}-\text{O})$
CFLH	1708	1624	1340	284	–	–
1	1620	1576	1372	204	544	515
2	1626	1581	1373	208	540	520
3	1627	1579	1361	212	537	509
4	1623	1561	1355	206	541	519
5	1619	1569	1362	207	539	518
6	1622	1577	1378	199	532	510
7	1624	1575	1364	211	536	516
8	1618	1580	1370	210	545	507

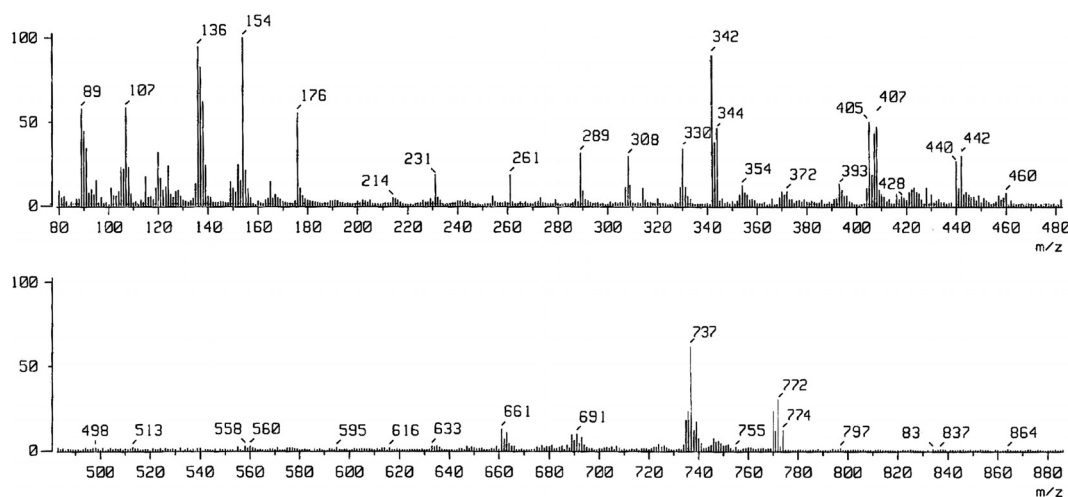


Figure 1. FAB-mass spectra of $[\text{Cu}(\text{CFL})(\text{A}^1)\text{Cl}] \cdot 2\text{H}_2\text{O}$ at the accelerating voltage was 10 kV.

ues in our case are very close to the spin-only values expected for $s = \frac{1}{2}$ system (1.73 BM), which lead a path to conclude that central metal atoms in synthesized complexes have one unpaired electron responsible for $s = \frac{1}{2}$ system.^[34]

Thermogravimetric Analysis

Thermogravimetric analysis was carried out at a heating rate of 10 K per minute in the range of 20–800 °C in a nitrogen atmosphere. The characteristic thermogravimetric curve (mass loss in % to temperature in °C) shows three distinct mass losses.^[35] Mass lost (approximately 4%) occurring during first decomposition step between 50–120 °C corresponds to loosely bind two molecules of crystallization water. The mass loss (approx. 42%) during second step between 180 to 300 °C corresponds to decomposition of neutral bidentate ligand, in which two coordination bonds are involved. The third step (approx. 41%) corresponds to decomposition of CFL, in which one coordination bond and one covalent bond are involved leaving behind the CuO (approx. 9%) as residue. So these three decomposition steps show ternary nature of the complexes.

The structure of complex **1**, assigned according to above analytical facts is shown in Figure 2.

Antibacterial Activity

The antibacterial efficiencies of the $\text{CuCl}_2 \cdot 2\text{H}_2\text{O}$, ligands, standard drugs, and the complexes were tested against two Gram(+ve) *Staphylococcus aureus*, *Bacillus subtilis*, and three Gram(–ve) *Serratia marcescens*, *Escherichia coli*, and *Pseudomonas aeruginosa* microorganisms in terms of MIC in μM . The minimum inhibitory concentration (MIC) is defined as the lowest concentration of antimicrobial agent showing complete inhibition of growth of microorganisms. The results concerning *in vitro* antibacterial activity (MIC) are presented in Table 2. The antimicrobial activity of all the complexes against the five microorganisms is much higher than that of $\text{CuCl}_2 \cdot 2\text{H}_2\text{O}$ and free ligands. The inhibition activity seems to

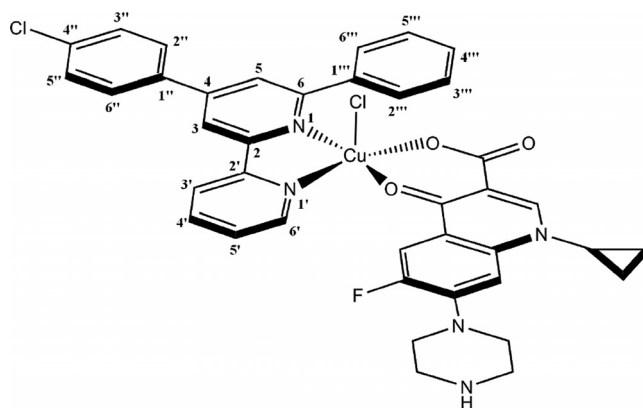


Figure 2. Proposed structure of complex **1**.

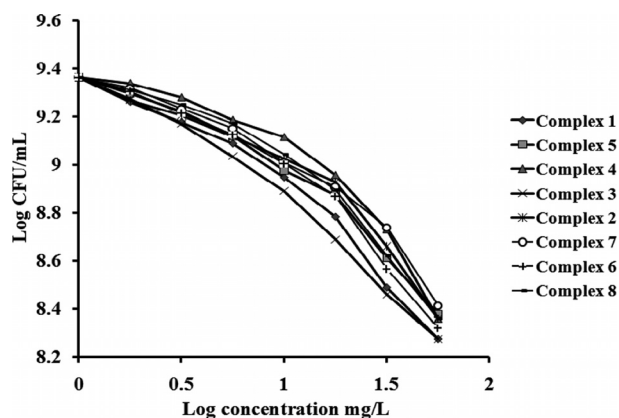
be governed in certain degree by the facility of coordination at the metal atom as well as electronic nature of the ligands. The biomolecular interaction with metal complexes can be the cause for inhibition of biological synthesis and this prevent the organisms from reproducing.^[28] The copper chelation with ligand reduces polarity of metal ion by overlap of the ligand orbital and partial sharing of the positive charge of the metal ion with the donor groups. Increase in delocalization of π electrons over the whole ligand enhances the penetration of complexes into lipid membranes and blocking of the metal binding sites in the enzymes of microorganisms. The complexes may also disturb the respiration process of the cell and thus block the synthesis of proteins, which restricts further growth of the organism and thus results in the overall gain in the biological potency. It has been proposed that quinolone in solution form the stable bonds with metal ion.^[36] Our data also supported the fact that metal ion is required for tight binding of DNA with quinolone,^[37] since synthesized metal complexes or chelates (metal bounded quinolone) show better antimicrobial activity than free quinolone.

In addition, our study regarding bactericidal activity in terms of CFU per mL of the metal complexes against same microorganisms reveal decrease in number of colonies with increasing

Table 2. MIC in terms of μM .

Compounds	Gram positive		Gram negative		
	<i>S. aureus</i>	<i>B. subtilis</i>	<i>S. marcescens</i>	<i>P. aeruginosa</i>	<i>E. coli</i>
$\text{CuCl}_2 \cdot 2\text{H}_2\text{O}$	2698.0	2815.0	2756.0	2404.0	3402.0
Ciprofloxacin	1.6	1.1	1.6	1.4	1.4
Gatifloxacin	5.1	4.0	2.9	1.0	2.9
Norfloxacin	2.5	2.5	4.1	3.8	2.8
Enrofloxacin	1.9	3.9	1.7	1.4	1.4
Pefloxacin	2.1	2.4	5.1	5.7	2.7
Levofloxacin	1.7	2.2	1.7	1.7	1.0
Sparfloxacin	1.3	2.0	1.5	1.5	1.3
Ofloxacin	1.9	1.4	1.7	2.2	1.4
A ¹	194.0	169.0	272.0	255.0	278.0
A ²	130.0	250.0	506.0	154.0	129.0
A ³	194.0	169.0	272.0	255.0	278.0
A ⁴	255.0	278.0	275.0	267.0	268.0
A ⁵	184.0	139.0	272.0	255.0	278.0
A ⁶	194.0	169.0	286.0	250.0	506.0
A ⁷	167.0	145.0	272.0	255.0	278.0
A ⁸	194.0	169.0	244.0	255.0	278.0
[Cu(CFL)(A ¹)Cl]·2H ₂ O (1)	0.7	0.5	1.8	1.5	1.5
[Cu(CFL)(A ²)Cl]·2H ₂ O (2)	1.6	0.4	0.8	1.8	1.6
[Cu(CFL)(A ³)Cl]·2H ₂ O (3)	1.7	0.3	0.7	1.3	1.4
[Cu(CFL)(A ⁴)Cl]·2H ₂ O (4)	0.8	1.8	0.8	1.5	1.5
[Cu(CFL)(A ⁵)Cl]·2H ₂ O (5)	2.1	2.3	2.1	2.1	2.0
[Cu(CFL)(A ⁶)Cl]·2H ₂ O (6)	1.5	1.8	1.4	0.5	1.7
[Cu(CFL)(A ⁷)Cl]·2H ₂ O (7)	0.7	0.3	0.3	0.5	1.6
[Cu(CFL)(A ⁸)Cl]·2H ₂ O (8)	1.6	0.6	1.0	1.2	1.6

the concentration of compounds. The results are shown in Figure 3 for all the complexes against *S. aureus*. The maximum concentration reveals bactericidal activity for all the complexes is 1.75 μM . The number of colonies counted in this technique was 30–250 CFU per mL.

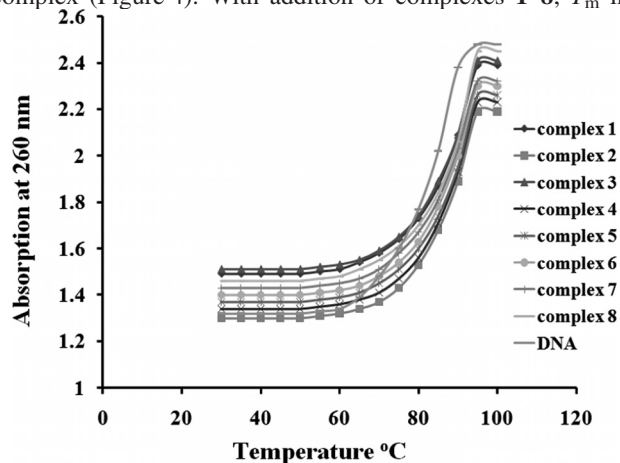
**Figure 3.** Relationship between concentration and bactericidal activity of all complexes against *S. aureus*.

Thermal Denaturation Studies

Thermal behaviors of DNA in the presence of complexes can give insight of their conformational changes when temperature is raised, and offer information about the interaction strength of complexes with DNA. It is well known that when the temperature of the solution increases, the double stranded DNA gradually dissociates to single strands and generates a

hyperchromic effect on the absorption spectra of DNA bases ($\lambda_{\text{max}} = 260 \text{ nm}$). In order to identify this transition process, the melting temperature T_m , which is defined as the temperature, where half of the total base pairs are unbound, is usually introduced. The binding of metal complexes to the double stranded DNA usually stabilizes the duplex structure to some extent depending on the strength of interaction with nucleic acid.^[38] The binding should lead to an increase in the melting temperature (T_m) of DNA as compared to DNA itself.

According to the literature the interaction of metallointercalators generally results in a considerable increase in melting temperature (T_m). DNA (100 μM) melting experiments reveal T_m of Herring sperm DNA $82.8 \pm 1 \text{ }^\circ\text{C}$ in the absence of the complex (Figure 4). With addition of complexes 1–8, T_m in-

**Figure 4.** Melting curves of herring sperm DNA in the absence and presence of complexes 1–8.

creased to 88.2 ± 1 °C, 86.5 ± 1 °C, 88.5 ± 1 °C, 86.7 ± 1 °C, 86.9 ± 1 °C, 87.5 ± 1 °C, 87.9 ± 1 °C and 88.0 ± 1 °C, respectively. The increased T_m (3.7–5.7 °C) value of the DNA after addition of the complexes is comparable to that observed for classical intercalators.^[39]

Viscosity Measurements

The arrangement of a supercoiled molecule may be altered by any factor, which affects the intrinsic twisting of the DNA helix. One important factor is the presence of an intercalator, e.g. ethidium bromide, the positively charged polycyclic aromatic compound, which binds to DNA by inserting itself between the base pairs. Intercalators introduce strong structural perturbations in DNA. The axial flexibility of DNA in the sense of dynamic flux of changes in axial and helical parameters allows the compound to stack between adjacent DNA base pair. The complex is thought to be stabilized by π - π stacking interactions between the compound and DNA bases. The possibility of bending the helix with larger ring systems and the steric restrictions on intercalation is supported by viscosity study. A classical intercalation model demands that the DNA helix lengthens as base pairs are separated to accommodate the complex, leading to the increase of DNA viscosity. In contrast, decrease in DNA viscosity is noted in the partial or non-classical intercalator like in ciprofloxacin, because it may bend (or kink) DNA helix, thereby decreasing its effective length. For all the complexes, as increasing the amounts of complexes, the viscosity of DNA increase steadily (Figure 5). Similar mechanism was suggested for the complexes $[\text{Ru}(\text{tpy})(\text{pta})]^{2+}$ and $[\text{Ru}(\text{tpy})(\text{ptp})]^{2+}$ reported by Chao et al.^[40]

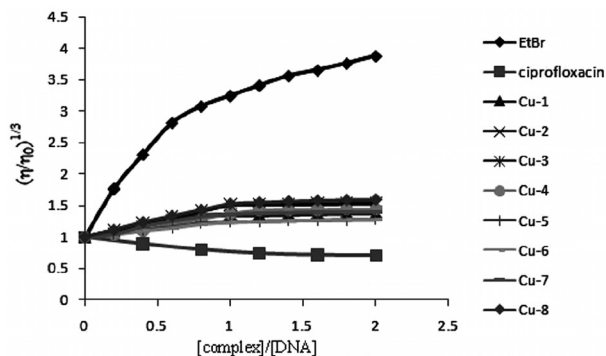


Figure 5. Viscometric curve for complexes showing classical intercalative mode of binding.

Absorption Titration

It is a general observation that the binding of intercalative molecules to DNA is accompanied by a red shift and hypochromism in the absorption spectra due to the strong stacking interaction between aromatic chromophore of the complex and the base pairs of DNA. The extent of spectral change is related to the strength of binding. The spectra for intercalators are more perturbed than those for groove binders.^[41]

All copper(II) complexes exhibit an intense absorption band around 274 nm, which is attributed to intraligand n - π^* or π - π^* transition of intercalative ligands. The increasing concentration of herring sperm DNA results in the obvious tendency of hypochromism with a bathochromic (approx. 4 nm) shift. To compare the binding strength of complexes quantitatively, the intrinsic binding constants K_b of the complexes were determined by monitoring the changes of absorbance at 274 nm with increasing concentration of herring sperm DNA (Figure 6). From the plot of $[\text{DNA}]/(\epsilon_a - \epsilon_f)$ versus $[\text{DNA}]$, the K_b value of all the complexes were found to be 1.14×10^4 to $1.67 \times 10^4 \text{ M}^{-1}$ (Table S1, Supporting Information). For each set of compounds, the spectral changes for the individual compounds differ only slightly from each other, which indicates that their interactions with DNA were similar and the complexes have comparable binding constant. The observed bathochromicity and hypochromicity suggest an intimate association of the complexes with DNA and also that the complexes may bind to the helix by intercalation. These values are comparable to that observed for $[\text{Ru}(\text{phen})(\text{phi})]^{2+}$ (2.72×10^4)^[42] and $[\text{Cu}(\text{erx})_2(\text{H}_2\text{O})]$ (3.12×10^4)^[43] but smaller than those observed for $[\text{Ru}(\text{bpy})(\text{dppz})]^{2+}$ ($> 10^6$)^[44]

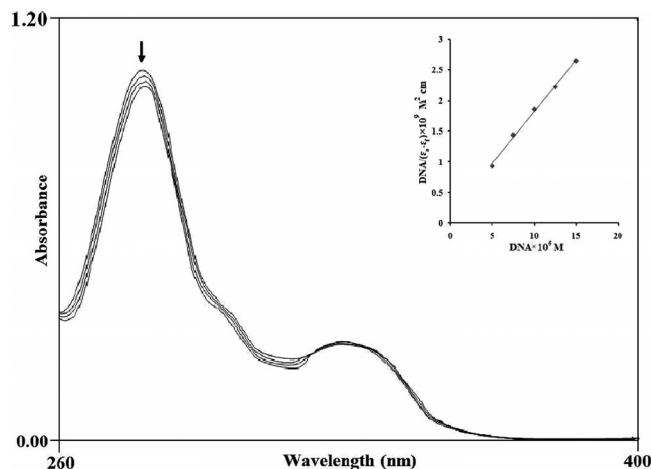


Figure 6. Electronic absorption spectra of $[\text{Cu}(\text{CFL})(\text{A}^1)\text{Cl}] \cdot 2\text{H}_2\text{O}$ (10 μM) in phosphate buffer ($\text{Na}_2\text{HPO}_4/\text{NaH}_2\text{PO}_4$, pH 7.2) in the absence and presence of increasing amount of DNA (50–150 μM). (Inset: Plot of $[\text{DNA}]/(\epsilon_a - \epsilon_f)$ versus $[\text{DNA}]$. Arrow shows the absorbance change upon increasing DNA concentrations).

Salt-dependence of Binding Constants

The typical plots of $[\text{DNA}]$ versus $[\text{DNA}]/(\epsilon_a - \epsilon_f)$ for determination of binding constant (K_b) of complex **1** to herring sperm DNA at various concentrations of NaCl based on Equation (1) (see Experimental Section) was used (Figure S2, Supporting Information). The detailed results are collected in Table 3. The reported binding constants are obtained over the concentration range 0.005 to 0.1 M NaCl, in order to apply polyelectrolyte theory to the calculation of the non-electrostatic binding constants and separate the binding free energy change into its electrostatic and nonelectrostatic contributions. The salt concentrations of 0.005–0.1 M were selected in this

study, because the polyelectrolyte theories are strictly applicable to salt concentrations of lower than 0.1 M. It has been reported that the dependence of K_b on salt concentration becomes non linear at higher concentrations of salt.^[45] The plot of $\ln[\text{Na}^+]$ against $\ln K_b$ for the binding of complex **1** to DNA is given in Figure 7. It is clear from the plots that the binding constant decreases with increasing salt concentration. This is due to the stoichiometric amount of ion release that follows the binding of charged ligand, i.e. copper(II) complex,^[46] suggesting that electrostatic interaction is involved in the DNA-binding event.

Table 3. Equilibrium binding constant (K_b) for the binding of complex **1** to herring sperm DNA in 0.2 M phosphate buffer (pH 7.2) at 25 °C and various concentrations of NaCl.

$[\text{Na}^+]/\text{M}$	$K_b/10^3/\text{M}^{-1}\text{ bp}$	$K_t^\circ/10^3/\text{M}^{-1}\text{ bp}$	$K_t^\circ/K_b/\%$
0.005	12.0	1.2	10.0
0.025	7.1	1.3	18.3
0.050	5.2	1.2	23.1
0.075	4.1	1.1	26.8
0.100	3.6	1.1	30.6

Average = $6.4 \pm 0.33 (10^3)$

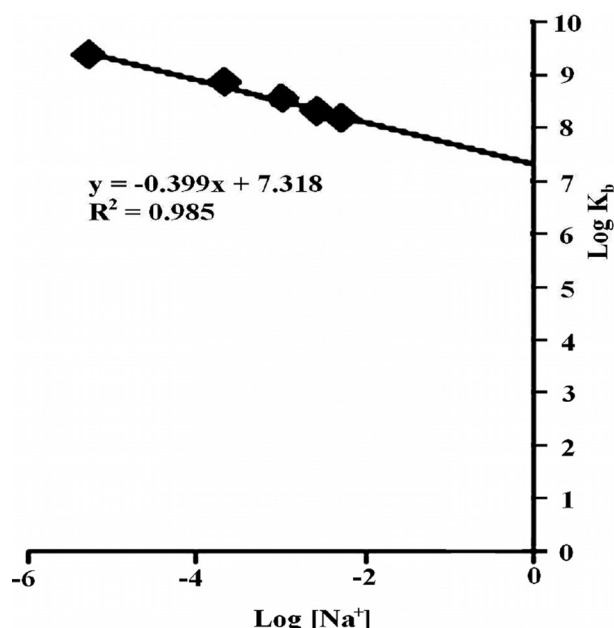


Figure 7. Salt dependence of binding constant (K_b) for the binding of complex **1** (10 μM) to herring sperm DNA.

Using the slope of linear fitting of Figure 7, we may calculate non-electrostatic binding constant (K_t°) at various concentrations of NaCl ($[\text{Na}^+]$) according to the following polyelectrolyte theory:^[46]

$$\ln K_b = \ln K_t^\circ + Z\xi^{-1} \{\ln(\gamma_{\pm}\delta)\} + Z\psi \ln[\text{Na}^+],$$

where $Z\psi$ is estimated from the slope of the regression line in Figure 7. Z is partial charge on the binding ligand involved in the DNA interaction as predicted by polyelectrolyte theory, ψ is the fraction of counterions associated with each DNA phosphate unit ($\psi = 0.88$ for double-stranded B-form DNA), γ_{\pm} is the mean activity coefficient at cation concentration of Na^+ ,

and the remaining terms are constants for double stranded DNA in B form, i.e. $\xi = 4.2$ and $\delta = 0.56$. Results of the calculations are summarized in Table 4 along with the percentage of K_t° contribution to the total binding constants (K_b) at various concentrations of Na^+ . The K_t° can be taken as a measure how large the non-electrostatic forces stabilize the ligand–DNA interaction. In contrast to the K_b values, which are salt-dependent, the magnitude of K_t° is constant throughout the concentration of NaCl employed with the average value of $1.18 \times 10^3 \text{ M}^{-1} \text{ bp}$. This is in agreement with the expectation for the salt-independency of this parameter. Although the values of K_t° are constant throughout the concentrations of salt, the percentage of K_t° contributions to the K_b increases significantly and reach a maximum of 30.6% at $[\text{Na}^+] = 0.1 \text{ M}$. It can be expected that at higher concentrations of salt, e.g. at physiological condition ($\text{Na}^+ \approx 0.2 \text{ M}$), the non-electrostatic forces would play a major role in the DNA binding of the copper(II) complex. The value of 23.1% for the non-electrostatic binding constant found in the DNA binding of complex **1** at NaCl = 0.05 M is considered to be high even when it is compared with those of other proven intercalators such as ethidium (12.3%) at the same ionic strength.^[47]

Table 4. Thermodynamic parameters for the binding of copper(II) complexes to herring sperm DNA at 0.005 M NaCl.

DNA Binders	$K_b/10^3/\text{M}^{-1}\text{ bp}$	ΔG°	SK	$\Delta G_{\text{pe}}^\circ$	$K_t^\circ/10^3 (\%K_t^\circ/K_b)/\text{M}^{-1}\text{ bp}$	$\Delta G_t^\circ (\% \Delta G_t^\circ/\Delta G^\circ)$
1	5.2	-21.2	0.399	-2.9	1.2 (23.1)	-18.3 (86.3)
2	4.3	-20.7	0.474	-3.5	0.9 (20.9)	-17.2 (83.1)
3	5.8	-21.4	0.360	-2.7	1.8 (31.0)	-18.7 (87.4)
4	4.5	-20.8	0.394	-2.9	1.2 (26.7)	-17.9 (86.1)
5	5.4	-21.2	0.323	-2.4	1.8 (33.3)	-18.8 (88.7)
6	5.6	-21.3	0.342	-2.5	1.8 (32.1)	-18.8 (88.3)
7	6.0	-21.5	0.318	-2.3	2.1 (35.0)	-19.2 (89.3)
8	5.8	-21.4	0.345	-2.5	1.8 (31.0)	-18.9 (88.3)
EtBr ^(a)	494	-32.2	0.75	-5.0	61.0 (12.3)	-27.2 (84.5)

a) Taken from reference.^[48]

By further analysis is also possible to dissect the binding free energy change (ΔG°) for the binding of complex **1** to DNA into its electrostatic ($\Delta G_{\text{pe}}^\circ$) and non-electrostatic (ΔG_t°) contributions at a given concentration of NaCl.^[44] Table 4 summarizes the results of energetics calculation for the binding of metal complexes to DNA in 0.05 M NaCl as well as proven organic intercalator, EtBr,^[46,48] for the purpose of comparison.

The total binding free energy changes listed in Table 4 were calculated based on the standard Gibbs relation:

$$\Delta G^\circ = -RT \ln[K_b]$$

where R is the gas constant and T is the temperature in Kelvin. The salt dependence of the binding constant is defined as the slope, SK.

The SK value can be used to calculate the polyelectrolyte contribution of the free energy change (ΔG_{pe}°) to the overall free energy change (ΔG°) at a given NaCl concentration by the relation:^[46,48]

$$\Delta G_{pe}^{\circ} = (SK) RT \ln[Na^{+}]$$

The difference between the Gibbs free energy change (ΔG°) and ΔG_{pe}° is defined as the non-electrostatic free energy change:

$$\Delta G_t^{\circ} = \Delta G^{\circ} - \Delta G_{pe}^{\circ}$$

The quantity ΔG_t° corresponds to the portion of the binding free energy change, which is independent of salt concentrations and contains a minimal contribution from polyelectrolyte effects such as coupled ion release.

DNA Cleavage Studies

There has been considerable interest in DNA cleavage reactions that are activated by transition metal complexes.^[49,50] Figure 8 illustrates the gel electrophoretic separations showing the cleavage of pUC19 DNA induced by the complexes under aerobic conditions.^[51] When circular plasmid DNA is conducted by electrophoresis, the fastest migration is observed for the supercoiled form (SC). If one strand is cleaved, the supercoiled will relax to produce a slower-moving open circular form (OC). If both strands are cleaved, a linear form (L) is generated that migrates in between. This clearly shows that the relative binding efficacy of the complexes to DNA is much higher than the binding efficacy of metal salt itself or ciprofloxacin (Table S2, Supporting Information). The different DNA-cleavage efficiency of the complexes was due to the different binding affinity of the complexes to DNA, which was observed in other cases. The involvement of reactive oxygen species (hydroxyl and singlet oxygen) in the nuclease mechanism can be inferred by monitoring of the quenching of the DNA cleavage in the presence of radical scavengers in solution. Complexes 1–8 do not show inhibition of DNA cleavage in the presence of scavengers of hydroxyl radicals (DMSO) (Figure S3, Supporting Information) and singlet oxygen (sodium azide) (Figure S4, Supporting Information). This indicates that the cleavage of DNA probably follows a hydrolytic cleavage mechanism. Hydrolytic DNA cleavage involves cleavage of phosphoester bond to generate fragments those could be subsequently relegated. Such DNA hydrolysis by copper(II) complexes have been reported earlier.^[52]

SOD: SOD-like Activity

Superoxide is one of the main reactive oxygen species (ROS) in the cell and as such, superoxide dismutase (SOD) serves a key antioxidant role. SOD outcompetes damaging reactions of superoxide, thus protecting the cell from superoxide toxicity. The reaction of superoxide with non-radicals is spin forbidden in biological systems; this means, its main reactions are with itself (dismutation) or with another biological radical such as nitric oxide (NO). The superoxide anion radical ($O_2^{\cdot-}$)

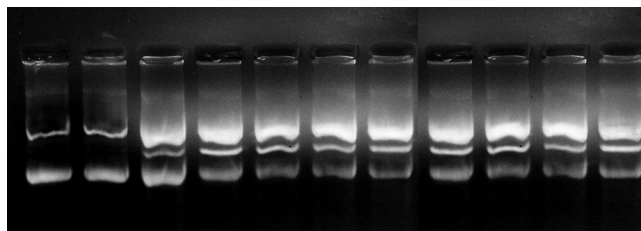


Figure 8. Photogenic view of cleavage of pUC19 DNA: Lane 1, DNA control; Lane 2, pUC19 DNA + $CuCl_2 \cdot 2H_2O$; Lane 3, pUC19 DNA + Ciprofloxacin; Lane 4, pUC19 DNA + $[Cu(CFL)(A^1)Cl] \cdot 2H_2O$; Lane 5, pUC19 DNA + $[Cu(CFL)(A^2)Cl] \cdot 2H_2O$; Lane 6, pUC19 DNA + $[Cu(CFL)(A^3)Cl] \cdot 2H_2O$; Lane 7, pUC19 DNA + $[Cu(CFL)(A^4)Cl] \cdot 2H_2O$; Lane 8, pUC19 DNA + $[Cu(CFL)(A^5)Cl] \cdot 2H_2O$; Lane 9, pUC19 DNA + $[Cu(CFL)(A^6)Cl] \cdot 2H_2O$; Lane 10, pUC19 DNA + $[Cu(CFL)(A^7)Cl] \cdot 2H_2O$; Lane 11, pUC19 DNA + $[Cu(CFL)(A^8)Cl] \cdot 2H_2O$.

spontaneously dismutates to O_2 and hydrogen peroxide (H_2O_2) quite rapidly (approx. $10^5 M^{-1}s^{-1}$ at pH 7). SOD is biologically necessary because superoxide reacts even faster with certain targets such as the NO radical, which makes peroxyntirite.

The system used as a source of superoxide radical generator was NBT/NADH/PMS system in order to check SOD like activity of the synthesized complexes. Copper is known to give good SOD activity, although their structure are totally unrelated with native enzyme.^[53] The IC_{50} value (chromophore require to yield 50% inhibition of the reduction of NBT) of the present complexes are lower than the value exhibit by the copper salt (Figure S5, Supporting Information). The copper(II) complexes showed SOD-like activity, which was evaluated by the scavenger concentration which causes 50% inhibition in the detector formation i.e. IC_{50} . Compounds exhibit SOD-like activity at biological pH with their IC_{50} values ranging from 0.6 to 1.3 μM . The superoxide scavenging data (Table S3, Supporting Information) suggest that all the complexes are active compared to the complexes of type $[Cu(\text{sulfathiazole})(py)_3Cl]$ (1.31–5.17 μM) reported by Casanova et al.^[54] The lower IC_{50} can only be accredited to the vacant coordination, which facilitates the binding of superoxide anion, electrons of aromatic ligands that stabilize $Cu-O_2^{\cdot-}$ interaction and not only to the partial dissociation of complex in solution. Copper(II) complexes mimic the SOD enzyme and bind with $O_2^{\cdot-}$ at its vacant coordinating site resulting in formation of octahedral arrangement (Figure S6, Supporting Information). The interaction mechanism could involve a direct attack of the $O_2^{\cdot-}$ ion on the free axial position of the Cu^{II} ion passing through a six-coordinate adduct, which is highly unstable due to the Jahn–Teller effect.^[55] As a consequence of this interaction, the central metal ion Cu^{II} undergoes rapid reduction to Cu^I . It is assumed that electron transfer between the central metal and $O_2^{\cdot-}$ occurs by direct binding.^[56]

Conclusions

The spectroscopic data suggests square pyramidal arrangement for all the complexes. The Cu^{II} complexes mimic the SOD enzyme and mechanism suggests transformation of

square pyramidal – octahedral arrangement, while scavenging superoxide radicals. The effect of Cu^{II} coordination in enhancing the antimicrobial properties is clearly visualized by MIC data as the resulting complexes are more bacteriostatic even than standard tested drugs. Additionally biocidal activity shows decrease in number of colonies as compound concentration increases. The viscometry data are in good agreement with bathochromicity and hypochromicity observed in UV/Vis absorption curve and suggests classical intercalation for all the complexes. The above DNA interaction data are well supported by thermal denaturation study. The gel electrophoresis experiments validate again sufficient interaction between DNA and Cu^{II} complexes and gel electrophoresis in presence of radical scavenging agents suggest the hydrolytic cleavage mechanism for plasmid DNA. The thermodynamic profile of complex–DNA interaction is illustrated as binding free energy by absorption data. The effect of increasing salt concentration is clearly visualized and suggests electrostatic interaction existence in presence of electrolytic material.

Experimental Section

Materials and Methods: All the chemicals and solvent used were of analytical grade. Ciprofloxacin hydrochloride was purchased from Bayer AG, Wuppertal, Germany. Pyridine, 2-acetyl pyridine, *p*-chloro benzaldehyde, *m*-chloro benzaldehyde, *p*-bromo benzaldehyde, *m*-bromo benzaldehyde, *p*-fluoro benzaldehyde, *p*-methyl benzaldehyde, *p*-methoxy benzaldehyde, and *p*-benzyloxy benzaldehyde were purchased from Loba Chemie Pvt. Ltd., India. Ethidium bromide and Luria Broth were purchased from Himedia, India. Acetic acid and EDTA were purchased from Sd fine Chemicals, India. Herring sperm DNA was purchased from Sigma Chemical Co., India.

Instrumentation: IR spectra were recorded with a FT-IR Shimadzu spectrophotometer with sample prepared as KBr pellets in the range 4000–400 cm⁻¹. C, H, and N elemental analyses were performed with a model Perkin–Elmer 240 elemental analyzer. The metal contents of the complexes were analyzed by EDTA titration^[57] after decomposing the organic matter with a mixture of HClO₄, H₂SO₄, and HNO₃ (1:1.5:2.5). MIC study was carried out by means of laminar air flow cabinet, Toshiba, Delhi, India. Thermogravimetric analyses was obtained with a model 5000/2960 SDTA, TA instrument (USA). The ¹H NMR and ¹³C NMR were recorded with a Bruker Avance (400 MHz). The electronic spectra were recorded with a UV-160A UV/Vis. spectrophotometer, Shimadzu (Japan). The magnetic moments were measured by Gouy's method using mercury tetrathiocyanatocobaltate(II) as the calibrant ($\chi_g = 16.44 \times 10^{-6}$ cgs units at 20 °C), Citizen Balance. The diamagnetic correction was made using Pascal's constant. The FAB mass spectra were recorded with a Jeol SX 120/Da-600 mass spectrometer/ data system using argon/xenon (6 kV, 10 mA) as the FAB gas. The accelerating voltage was 10 kV and spectra were recorded at room temperature.

Synthesis of Ligands

Ligands A¹–A⁸ were prepared by reaction of the appropriate enone with pyridinium salt.^[58] The following procedure is for typical preparation along with their ¹H NMR and ¹³C NMR spectroscopic assignments and analytical data.

4-(4-Chlorophenyl)-6-phenyl-2,2'-bipyridine (A¹): An excess of ammonium acetate (approx. 10 equiv.) was added to a mixture of 1-(2-

pyridyl)-3-(4-chlorophenyl)propen-1-one (1.5 mmol) and 1-[2-oxo-2-(pyridyl)ethyl]pyridinium iodide (1.5 mmol) in methanol (20 mL). After heating to reflux for 5–7 h, the reaction mixture was allowed to cool, which led to the formation of greenish yellow needles of pure product. The solid was filtered off, washed with cold methanol, and dried under vacuum. Yield 51.3%, m.p. 140 °C. Anal. C₂₂H₁₅ClN₂ (342.82): calcd. C 77.87; H 4.41; N 8.17%; found: C 77.58; H 4.55; N 7.99%. ¹H NMR (CDCl₃, 400 MHz): $\delta = 8.754$ – 8.710 (complex, 2 H, H3',6'), 8.659 (s, 1 H, H3), 8.220 (d, 2 H, H2''',6'''), 7.960 (s, 1 H, H5), 7.910 (t, 1 H, H4'), 7.789 (d, 2 H, H2'',6''), 7.578–7.474 (complex, 5 H, H3'',5'',3''',4''',5'''), 7.386 (t, 1 H, H5') ppm. ¹³C NMR (CDCl₃, 100 MHz): $\delta = 157.43$ (C2), 155.86 (C2'), 150.22 (C6), 149.09 (C4), 147.22 (C6'), 139.28 (C1''), 138.25 (C1'''), 137.08 (C4'), 135.30 (C4''), 129.30 (C2''',6'''), 128.80 (C2'',6''), 128.55 (C3''',5'''), 127.10 (C3'',5''), 124.08 (C4'), 121.78 (C5'), 118.40 (C3'), 117.50 (C3), 102.75 (C5) ppm.

6-Phenyl-4-*p*-tolyl-2,2'-bipyridine (A²): A similar procedure was followed by taking 1-(2-pyridyl)-3-(4-tolyl)propen-1-one as enone. Yield 56.4%, m.p. 121 °C. Anal. C₂₃H₁₈N₂ (322.40): calcd. C 85.68; H 5.63; N 8.69%; found: C 85.83; H 5.51; N 8.77%. ¹H NMR (CDCl₃, 400 MHz): $\delta = 8.776$ – 8.723 (complex, 3 H, H3,3',6'), 8.232 (dd, 2 H, H2''',6'''), 8.020 (s, 1 H, H5), 7.934 (t, 1 H, H4'), 7.787 (d, 2 H, H2'',6''), 7.560 (t, 2 H, H3''',5'''), 7.485 (t, 1 H, H4''), 7.404 (t, 1 H, H5'), 7.358 (d, 2 H, H3'',5''), 2.446 (s, 3 H, CH3) ppm. ¹³C NMR (CDCl₃, 100 MHz): $\delta = 157.20$ (C2), 156.05 (C2'), 155.47 (C6), 150.27 (C4), 148.41 (C6'), 139.52 (C1''), 139.18 (C1'''), 137.56 (C4'), 135.63 (C4''), 129.80 (C3''',5'''), 129.12 (C3''',5'''), 128.77 (C2''',6'''), 127.12 (C2'',6'',4''), 123.88 (C5'), 121.85 (C3'), 118.47 (C3), 117.53 (C5), 21.29 (CH3) ppm.

4-(4-Bromophenyl)-6-phenyl-2,2'-bipyridine (A³): A similar procedure was followed by taking 1-(2-pyridyl)-3-(4-bromophenyl)propen-1-one as enone. Yield 51.7%, m.p. 146 °C. Anal. C₂₂H₁₅BrN₂ (387.27): calcd. C 68.23; H 3.90; N 7.23%; found: C 68.36; H 4.05; N 7.08%. ¹H NMR (CDCl₃, 400 MHz): $\delta = 8.882$ (s, 1 H, H3), 8.828–8.806 (complex, 2 H, H3',6'), 8.201 (dd, 2 H, H2''',6'''), 8.091 (t, 1 H, H4'), 8.009 (d, 1 H, H5), 7.807 (d, 2 H, H2'',6''), 7.683 (d, 2 H, H3'',5''), 7.578–7.482 (complex, 4 H, H5',3''',4''',5''') ppm. ¹³C NMR (CDCl₃, 100 MHz): $\delta = 157.83$ (C2), 154.42 (C2') 149.48 (C6), 146.61 (C4), 143.55 (C6'), 139.75 (C1''), 138.85 (C1'''), 137.00 (C4'), 132.36 (C2''',6'''), 129.48 (C4'''), 128.94 (C2'',6''), 128.87 (C3''',5'''), 127.11 (C3'',5''), 124.52 (C4'), 123.87 (C5'), 122.92 (C3'), 118.92 (C3), 118.26 (C5) ppm.

4-(4-Methoxyphenyl)-6-phenyl-2,2'-bipyridine (A⁴): A similar procedure was followed by taking 1-(2-pyridyl)-3-(4-methoxyphenyl)propen-1-one as enone. Yield 48.5%, m.p. 107 °C. Anal. C₂₃H₁₈N₂O (338.40): calcd. C 81.63; H 5.36; N 8.28%; found: C 81.50; H 5.49; N 8.40%. ¹H NMR (CDCl₃, 400 MHz): $\delta = 8.797$ – 8.747 (complex, 3 H, H3,3',6'), 8.217 (dd, 2 H, H2''',6'''), 8.000–7.978 (complex, 2 H, H5,4'), 7.860 (d, 2 H, H2'',6''), 7.555 (t, 2 H, H3''',5'''), 7.502–7.441 (complex, 2 H, H5',4'''), 7.071 (d, 2 H, H3'',5''), 3.907 (s, 3 H, OCH₃) ppm. ¹³C NMR (CDCl₃, 100 MHz): $\delta = 160.78$ (C4''), 157.58 (C2), 157.12 (C2'), 153.48 (C6), 150.16 (C4), 146.73 (C6'), 139.22 (C1'''), 137.22 (C4'), 130.32 (C1''), 129.25 (C4'''), 128.81 (C2'',6''), 128.62 (C3''',5'''), 127.14 (C2''',6'''), 124.35 (C5'), 122.84 (C3'), 118.62 (C3), 117.93 (C5), 114.57 (C3'',5''), 55.43 (OCH₃) ppm.

4-(4-Benzyloxyphenyl)-6-phenyl-2,2'-bipyridine (A⁵): A similar procedure was followed by taking 1-(2-pyridyl)-3-(4-benzyloxyphenyl)propen-1-one as enone. Yield 53.3%, m.p. 117 °C. Anal. C₂₉H₂₂N₂O (414.50): calcd. C 84.03; H 5.35; N 6.76%; found: C 84.20; H 5.50; N 6.88%. ¹H NMR (CDCl₃, 400 MHz): $\delta = 8.793$

(complex, 3 H, H₃,3',6'), 8.222 (dd, 2 H, H₂'',6''), 8.006 (complex, 2 H, H₅,4'), 7.877 (complex, 2 H, H₂'',6''), 7.558 (t, 2 H, H₃'',5''), 7.507–7.375 (complex, 7 H, H₅',4''',Bz2,3,4,5,6), 7.151 (d, 2 H, H₃'',5''), 5.172 (s, 2 H, OCH₂) ppm. ¹³C NMR (CDCl₃, 100 MHz): δ = 159.84 (C4'), 157.37 (C2), 156.82 (C2'), 154.28 (C6), 149.81 (C4), 147.93 (C6'), 139.48 (C1'''), 137.29 (C4'), 136.76 (CBz1), 134.52 (C1''), 129.15 (C2'',6''), 129.08 (C3''',5'''), 128.76 (CBz3,5), 128.66 (CBz4), 128.09 (C4'''), 127.52 (C2''',6'''), 127.09 (CBz2,6), 123.95 (C5'), 122.15 (C3'), 118.26 (C3), 116.44 (C5), 115.44 (C3'',5''), 70.16 (OCH₂) ppm.

4-(3-Chlorophenyl)-6-phenyl-2,2'-bipyridine (A⁶): A similar procedure was followed by taking 1-(2-pyridyl)-3-(3-chlorophenyl)propen-1-one as enone. Yield 54.1%, m.p. 117 °C. Anal. C₂₂H₁₅ClN₂ (342.82): calcd. C 77.87; H 4.41; N 8.17%; found: C 77.69; H 4.58; N 8.29. ¹H NMR (CDCl₃, 400 MHz): δ = 8.780–8.708 (complex, 3 H, H₃,3',6'), 8.225(d, 2 H, H₂'',6''), 7.954 (complex, 2 H, H₅,4'), 7.840 (s, 1 H, H₂''), 7.760 (dd, 1 H, H₆''), 7.564 (complex, 2 H, H₄'',5''), 7.514–7.450 (complex, 3 H, H₃'',4''',5'''), 7.427 (dt, 1 H, H₅') ppm. ¹³C NMR (CDCl₃, 100 MHz): δ = 157.51 (C2), 155.78 (C2')148.96 (C6), 148.48 (C4), 143.56 (C6'), 140.59 (C1'''), 139.12 (C1'''), 137.62 (C4'), 135.16 (C3''), 130.39 (C4'')129.32 (C5''), 129.07 (C2''), 128.81 (C2''',6'''), 127.45 (C4'''), 127.16 (C3''',5'''), 125.54 (C6''), 124.08 (C5'), 121.91 (C3'), 118.61 (C3), 117.65 (C5) ppm.

4-(3-Bromophenyl)-6-phenyl-2,2'-bipyridine (A⁷): A similar procedure was followed by taking 1-(2-pyridyl)-3-(3-bromophenyl)propen-1-one as enone. Yield 49.7%, m.p. 132 °C. Anal. C₂₂H₁₅BrN₂ (387.27): calcd. C 68.23; H 3.90; N 7.23%; found: C 68.40; H 3.75; N 7.06%. ¹H NMR (CDCl₃, 400 MHz): δ = 8.763–8.714 (complex, 2 H, H₃,3',6'), 8.650 (s, 1 H, H₃), 8.231 (d, 2 H, H₂'',6''), 7.990 (s, 1 H, H₅), 7.960 (s, 1 H, H₂''), 7.912 (t, 1 H, H₄''), 7.780 (d, 1 H, H₆''), 7.620 (d, 1 H, H₄''), 7.565 (t, 2 H, H₃'',5''), 7.496 (t, 1 H, H₄''), 7.436–7.376 (complex, 2 H, H₅',5'') ppm. ¹³C NMR (CDCl₃, 100 MHz): δ = 157.60 (C2), 154.92 (C2'), 149.00 (C6), 148.44 (C4), 143.19 (C6'), 140.70 (C1''), 139.10 (C1'''), 135.76 (C4'), 132.08 (C3''), 130.68 (C2''), 130.25 (C5''), 129.40 (C4''), 128.83 (C2''',6'''), 127.13 (C4'''), 126.10 (C3''',5'''), 124.28 (C6''), 123.23 (C5'), 122.23 (C3'), 118.78 (C3), 117.93 (C5) ppm.

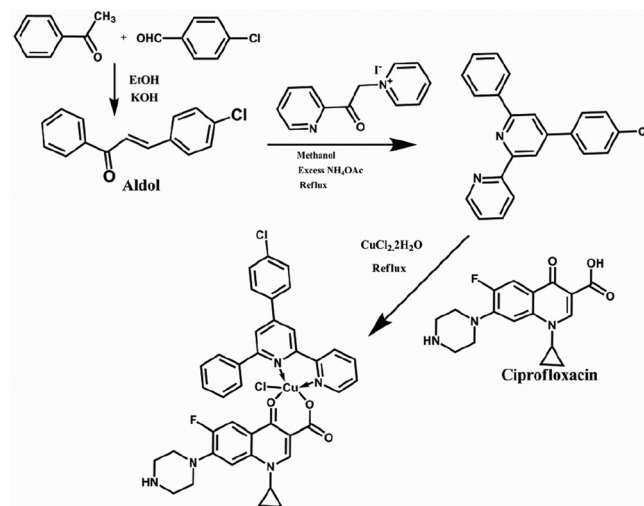
4-(4-Fluorophenyl)-6-phenyl-2,2'-bipyridine (A⁸): Similar procedure was followed by taking 1-(2-pyridyl)-3-(4-fluorophenyl)propen-1-one as enone. Yield 52.4%, m.p. 126 °C. Anal. C₂₂H₁₅FN₂ (326.37): calcd. C 80.96; H 4.63; N 8.58%; found: C 80.77; H 4.52; N 8.41%. ¹H NMR (CDCl₃, 400 MHz): δ = 9.092 (s, 1 H, H₃), 8.938–8.899 (complex, 2 H, H₃,3',6'), 8.266 (t, 1 H, H₄''), 8.203 (dd, 2 H, H₂'',6''), 8.074 (s, 1 H, H₅), 8.015 (dd, 2 H, H₂'',6''), 7.700 (t, 1 H, H₅'), 7.590–7.498 (complex, 3 H, H₃'',4''',5'''), 7.258 (t, 2 H, H₃'',5'') ppm. ¹³C NMR (CDCl₃, 100 MHz): δ = 164.79 (C4'), 157.46 (C2), 155.39 (C2'), 154.93 (C6), 149.43 (C4), 147.86 (C6'), 139.17 (C1'''), 138.29 (C1''), 134.56 (C4'), 129.29 (C2'',6''), 129.06 (C3''',5'''), 127.10 (C2''',6'''), 124.17 (C4'''), 122.22 (C5'), 118.63 (C3'), 117.84 (C3), 116.19 (C5), 115.98 (C3'',5'') ppm.

Synthesis of Complexes

[Cu(CFL)(A¹)Cl]·2H₂O (1): A methanol solution of CuCl₂·2H₂O (1.5 mmol) was added to methanol solution of 4-(4-chlorophenyl)-6-phenyl-2,2'-bipyridine (1.5 mmol), followed by addition of a previously prepared solution of ciprofloxacin (1.5 mmol) in methanol in presence of CH₃ONa (1.5 mmol). The pH was adjusted at 6.8 using dilute solution of CH₃ONa. The resulting solution was refluxed for 2 h on a water bath, followed by concentrating it to half of its volume.

A fine amorphous product of green color was obtained, which was washed with diethyl ether/hexane and dried in vacuo desiccator. Yield 67.8%, m.p. 225 °C. Anal. C₃₉H₃₆Cl₂CuFN₅O₅ (808.22): calcd. C 57.67; H 4.96; N 8.62; Cu 7.82%; found: C 57.85; H 4.85; N 8.70; Cu 7.85%.

In similar way, complexes **2–8** were prepared with the use of the corresponding ligands. The proposed reaction scheme is shown in Scheme 1.



Scheme 1. Reaction scheme for ligand (A¹) and complex 1.

[Cu(CFL)(A²)Cl]·2H₂O (2): It was prepared using 6-phenyl-4-p-tolyl-2,2'-bipyridine (1.5 mmol). Yield 66.4%, m.p. 215 °C. Anal. C₄₀H₃₉ClCuFN₅O₅ (788.72): calcd. C 60.68; H 5.47; N 8.84; Cu 8.03%; found: C 60.59; H 5.55; N 8.76; Cu 8.17%.

[Cu(CFL)(A³)Cl]·2H₂O (3): It was prepared using 4-(4-bromophenyl)-6-phenyl-2,2'-bipyridine (1.5 mmol). Yield 61.92%, m.p. 236 °C. Anal. C₃₉H₃₆BrClCuFN₅O₅ (852.67): calcd. C 54.68; H 4.71; N 8.18; Cu 7.42%; found: C 54.51; H 4.82; N 8.31; Cu 7.35%.

[Cu(CFL)(A⁴)Cl]·2H₂O (4): It was prepared using 4-(4-methoxyphenyl)-6-phenyl-2,2'-bipyridine (1.5 mmol). Yield 65.2%, m.p. 217 °C. Anal. C₄₀H₃₉ClCuFN₅O₆ (803.80): calcd. C 59.47; H 5.37; N 8.67; Cu 7.87%; found: C 59.55; H 5.49; N 8.60; Cu 7.99%.

[Cu(CFL)(A⁵)Cl]·2H₂O (5): It was prepared using 4-(4-(benzyloxy)phenyl)-6-phenyl-2,2'-bipyridine (1.5 mmol). Yield 71.3%, m.p. 206 °C. Anal. C₄₆H₄₃ClCuFN₅O₆ (879.8): calcd. C 62.74; H 4.89; N 7.96; Cu 7.22%; found: C 62.88; H 4.73; N 7.85; Cu 7.35%.

[Cu(CFL)(A⁶)Cl]·2H₂O (6): It was prepared using 4-(3-chlorophenyl)-6-phenyl-2,2'-bipyridine (1.5 mmol). Yield 66.7%, m.p. 220 °C. Anal. C₃₉H₃₆Cl₂CuFN₅O₅ (808.22): calcd. C 57.67; H 4.96; N 8.62; Cu 7.82%; found: C 57.80; H 4.83; N 8.76; Cu 7.67%.

[Cu(CFL)(A⁷)Cl]·2H₂O (7): It was prepared using 4-(3-bromophenyl)-6-phenyl-2,2'-bipyridine (1.5 mmol). Yield 62.2%, m.p. 232 °C. Anal. C₃₉H₃₆BrClCuFN₅O₅ (852.67): calcd. C 54.68; H 4.71; N 8.18; Cu 7.42%; found: C, 54.81; H 4.83; N 8.04; Cu 7.31%.

[Cu(CFL)(A⁸)Cl]·2H₂O (8): It was prepared using 4-(4-fluorophenyl)-6-phenyl-2,2'-bipyridine (1.5 mmol). Yield 69.5%, m.p. 218 °C. Anal. C₃₉H₃₆ClCuF₂N₅O₅ (791.76): calcd. C 58.86; H 5.07; N 8.80; Cu 7.99%; found: C 58.67; H 5.25; N 8.93; Cu 8.11%.

Antibacterial Activity: The MIC was determined using two fold serial dilutions in liquid media, of the compound being tested against control with no active ingredients, taking DMSO as the solvent. All equipment and culture media were sterilized. The incubation conditions comprise Luria Broth as media for culturing of bacteria at 37 °C. This culture was used as a control to examine if the growth of the bacteria tested was normal. In a similar second set, 20 µL of the bacterial solution as well as the tested compound at the desired concentration were added. We monitored bacterial growth by measuring the turbidity of the culture after 18 h. If a certain concentration of a compound inhibited bacterial growth, half the concentration of the compound was tested. This procedure was carried on to a concentration for bacteria grown normally. The lowest concentration that inhibited bacterial growth was determined as the MIC value.

The bactericidal action of all compounds was also evaluated against same bacterial culture. The inoculum was prepared by diluting an overnight culture grown in Luria Broth to obtain 10^6 viable bacteria·mL⁻¹ confirmed in each experiment by colony counts. Bacteria were exposed to concentrations of 0.25–1.75 µg·mL⁻¹ of compounds. The final volume was 1 mL. Cultures were incubated at 37 °C for 2 h. The 100 µL bacterial culture from above was taken and spread over previously prepared agar plate. These were incubated for 24 h at 37 °C and the visual colonies were calculated in order to check biocidal activity of metal complexes, yielding 30–250 colonies.

DNA Melting Temperature: Thermal denaturation studies were performed with a Perkin–Elmer Lambda 35 spectrophotometer equipped with a Peltier temperature-controlling programmer (± 0.1 °C). The absorbance at 260 nm was continuously monitored for solutions of Herring sperm DNA (100 µM) in the absence and the presence of complex (20 µM). The temperature of the solution was increased by 1 °C·min⁻¹.

Viscosity Measurement: Viscosity measurements were carried out using an Ubbelohde viscometer thermostatted at 27.0 ± 0.1 °C. Flow time was measured with a digital stopwatch, three times for each sample and an average flow time was calculated. Data are presented as $(\eta/\eta_0)^{1/3}$ versus binding ratio,^[59] where η and η_0 are the viscosity of DNA in the presence and in absence of the complex respectively. Viscosity values were calculated from the observed flow time of DNA-containing solutions ($t > 100$ s) corrected for the flow time of buffer alone (t_0): $\eta = t - t_0$.

Absorption Titration: A solution of herring sperm DNA in 0.2 M phosphate buffer (Na₂HPO₄ / NaH₂PO₄, pH 7.2) gave A₂₆₀/A₂₈₀ ratio 1.82 UV absorbance indicated that DNA was sufficiently free of protein. So, no further effort was made on purifying the commercially obtained DNA. The concentration of DNA was determined by absorption spectroscopy having ϵ value of 12858 mol⁻¹·cm⁻¹·L⁻¹ at 260 nm.^[60]

Spectroscopic titrations were carried out at room temperature to determine the binding affinity between DNA and the metal complex. The solutions of varying concentration of DNA (50–150 µM) and metal complexes (10 µM) were prepared along with blank sample of buffered DNA solution. After the solutions were mixed for 10 min, the absorption spectra were recorded. The titration processes were repeated until there was no change in the spectra for four titrations at least, indicating that binding saturation was achieved. Afterwards, the observed data were utilized to acquire the intrinsic binding constant, K_b using Equation (1):^[61]

$$[\text{DNA}]/(\epsilon_a - \epsilon_f) = [\text{DNA}]/(\epsilon_b - \epsilon_f) + 1/K_b (\epsilon_b - \epsilon_f) \quad (1)$$

where [DNA] is the concentration of DNA in terms of nucleotide phosphate [NP], ϵ_a , ϵ_f , and ϵ_b are the apparent, free and bound metal complex extinction coefficients respectively. K_b is the ratio of the slope to the y-intercept.

Measurements of Salt Dependence in DNA Binding: The salt dependent equilibrium binding constant (K_b) of copper(II) complex to herring sperm DNA was determined by spectrophotometric titration over the concentration range 0.005 to 0.100 M NaCl. A fixed amount of copper(II) complex in 0.2 M phosphate buffer at pH 7.2 and various concentrations of NaCl was titrated with increasing amounts of DNA stock solutions. The hypochromicity and bathochromicity due to metal complex–DNA interaction was monitored by UV-VIS spectrophotometer. The K_b values at various NaCl concentrations were calculated on the basis of Equation (1).

The salt concentration dependence of K_b for the DNA binding of the copper(II) complexes was evaluated by plotting $\ln K_b$ versus $\ln[\text{Na}^+]$ to obtain SK value, which is essential for polyelectrolyte analysis. Each measured point was the average value of at least three separate measurements with a relative standard deviation (RSD) normally less than 15%.

Gel Electrophoresis: Isolation of plasmid DNA from pure culture of *E. coli* was carried out by conventional method.^[62] The basic principle employed is “alkali-lysis”, in which at the alkaline pH, both the genomic and plasmid DNA are denatured. On reduction of the pH the plasmid DNA molecule being small in size, quickly reanneals itself, while the large genomic DNA is not. The denatured genomic DNA is sedimented, while the plasmid DNA remains in solution. Subsequently, this is precipitated.

For the gel electrophoresis experiments, supercoiled pUC19 DNA in TE buffer was treated with different Cu^{II} complexes; and in the presence of peroxide hydrogen in the reaction solution. The samples were incubated for 30 min at 37 °C and a loading buffer containing 10 mmol TE (pH 7.5), 0.03 % bromophenol blue, 0.03 % xylene cyanol FF, 60 % glycerol, and 60 mmol EDTA was added and electrophoresis was performed at 100 V for 2 h in TAE buffer using 1.0 % agarose gel containing 0.5 µg·mL⁻¹ ethidium bromide. Bands were visualized by UV light and photographed on a capturing system (AlphaDigiDoc™ RT. Version V.4.1.0 PC-Image software). For mechanistic investigations, experiments were carried out in the presence of radical scavenging agents, viz., DMSO (OH· radical) and NaN₃ (¹O₂ radical), which were added to SC DNA prior to the addition of the complex.

Determination of SOD-Like Activity: SOD-like activity of the investigated complexes was assayed using phenazemethosulfate (PMS) to photogenerate a reproducible and constant flux of superoxide anion radicals at pH = 7.2 (phosphate buffer). Reduction of nitroblue tetrazolium to blue formazan was used as an indicator of O₂⁻ production and followed spectrophotometrically at 560 nm by the addition of PMS (30 µM) to an aqueous solution of NBT (75 µM), NADH (79 µM), 0.25 to 2.0 µM complex solution and phosphate buffer.^[63] The reaction in blank samples and in the presence of copper complexes was measured for 5 min. The plot of time t against varying concentration of complex is drawn.

Supporting Information (see footnote on the first page of this article): Mass fragmentation pattern of compound; DNA binding constant and IC50 value of compounds; DNA cleavage data; plots for salt concentration effect on DNA binding and % inhibition of NBT reduction; gel images for gel electrophoresis experiment in presence of radical scavenging agents; and mechanism for damaging effect of ROS are provided.

Acknowledgement

We thank the Authority Head, Department of Chemistry, Sardar Patel University, Vallabh Vidyanagar, Gujarat, India for providing the laboratory facilities. Authors would also like to acknowledge U.G.C. for providing financial assistance of UGC grant 32-226/2006(SR).

References

- [1] B. Chen, S. Wu, A. Li, F. Liang, X. Zhou, X. Cao, Z. He, *Tetrahedron* **2006**, *62*, 5487.
- [2] H. Kamal, N. Shankaraiah, C. R. Reddy, S. Prabhakar, N. Markandeya, H. K. Shrivastava, G. N. Sastry, *Tetrahedron* **2010**, *66*, 5498.
- [3] M. S. Arias, G. A. Marta, M. J. Fernandez, A. Lorente, G. Alzuet, J. Borrás, *J. Inorg. Biochem.* **2009**, *103*, 1067.
- [4] R. Jacques, V. Antoine, P. Philippe, B. Jacques, *Crit. Rev. Oncol. Hemat.* **2004**, *51*, 205.
- [5] K. Jiao, Q. X. Wang, W. Sun, F. F. Jian, *J. Inorg. Biochem.* **2005**, *99*, 1369.
- [6] L. Ronconi, P. J. Sadler, *Coord. Chem. Rev.* **2007**, *251*, 1633.
- [7] J. L. Hall, *J. Exp. Bot.* **2002**, *53*, 1.
- [8] M. F. Reedijk, J. Arsic, D. Kaminski, P. Poodt, J. W. M. Van Kessel, W. J. Szweryn, H. Knops, E. Vlieg, *Phys. Rev. Lett.* **2003**, *90*, 56104.
- [9] D. S. Sigman, D. R. Graham, V. D. Aurora, A. M. Stern, *J. Biol. Chem.* **1979**, *254*, 12269.
- [10] G. Mendoza-Diaz, L. M. R. Martinez-Aguilera, R. Perez-Alonso, *Inorg. Chim. Acta* **1987**, *138*, 41.
- [11] G. Mendoza-Diaz, L. M. R. Martinez-Aguilera, R. Moreno-Esparza, K. H. Pannell, F. Cervantes-Lee, *J. Inorg. Biochem.* **1993**, *50*, 65.
- [12] S. C. Wallis, L. R. Gahan, B. G. Charles, T. W. Hambley, P. A. Duckworth, *J. Inorg. Biochem.* **1996**, *62*, 1.
- [13] E. K. Efthimiadou, H. Thomadaki, Y. Sanakis, C. P. Raptoulou, N. Katsaros, A. Scorilas, A. Karaliota, G. Psomas, *J. Inorg. Biochem.* **2007**, *101*, 64.
- [14] B. Macias, M. V. Villa, I. Rubio, A. Castineiras, J. Borrás, *J. Inorg. Biochem.* **2001**, *84*, 163.
- [15] J. D. Ranford, P. J. Sadler, D. A. Tocher, *J. Chem. Soc. Dalton Trans.* **1993**, *22*, 3393.
- [16] K. E. Erkkila, D. T. Odom, J. K. Barton, *Chem. Rev.* **1999**, *76*, 2777.
- [17] W. K. Pogozelski, T. D. Tullius, *Chem. Rev.* **1998**, *75*, 1089.
- [18] W. Bayer, J. Imlay, I. Fridovich, *Prog. Nucleic Acid Res. Mol. Biol.* **1991**, *31*, 221.
- [19] M. J. Robinson, B. A. Martin, T. D. Gootz, P. R. McGuirk, M. J. Osheroff, *Antimicrob. Agents Chemother.* **1992**, *36*, 751.
- [20] C. Sissi, M. Palumbo, *Curr. Med. Chem. Anti-Cancer Agents* **2003**, *3*, 43.
- [21] J. Hosomi, A. Maeda, Y. Oomori, T. Irikura, T. Yokota, *Rev. Infect. Dis.* **1988**, *10*, 148.
- [22] D. K. Chand, P. K. Bharadwaj, H. J. Schneider, *Tetrahedron* **2001**, *57*, 6727.
- [23] R. N. Patel, N. Singh, K. K. Shukla, J. Niclos-Gutierrez, A. Castineiras, V. G. Vaidyanathan, B. U. Nair, *Spectrochim. Acta* **2005**, *62*, 261.
- [24] P. K. Panchal, M. N. Patel, *Synth. React. Inorg. Met. Chem.* **2004**, *34*, 1277.
- [25] I. Leban, I. Turel, N. Bukovec, *J. Inorg. Biochem.* **1994**, *56*, 273.
- [26] K. Nakamoto, *Infrared and Raman Spectra of Inorganic and Coordination Compounds*, 4th ed., Wiley, New York, **1986**.
- [27] G. B. Deacon, R. J. Philips, *Coord. Chem. Rev.* **1980**, *23*, 227.
- [28] Z. H. Chohan, C. T. Suparan, A. Scozzafava, *J. Enz. Inhi. Med. Chem.* **2005**, *20*, 303.
- [29] I. Turel, I. Leban, N. Bukovec, *J. Inorg. Biochem.* **1997**, *66*, 241.
- [30] N. H. Patel, P. K. Panchal, P. B. Pansuriya, M. N. Patel, *J. Macro. Sci. Part A Pure Appl. Chem.* **2006**, *43*, 1083.
- [31] P. B. Pansuriya, P. Dhnadhukia, V. Thakkar, M. N. Patel, *J. Enz. Inhi. Med. Chem.* **2007**, *22*, 477.
- [32] H. H. Freedman, *J. Am. Chem. Soc.* **1961**, *83*, 2900.
- [33] M. Melnik, *Coord. Chem. Rev.* **1981**, *36*, 1.
- [34] B. N. Figgis, J. Lewis, in J. Lewis, R. G. Wilkins, *Modern Coordination Chemistry: Principles and Methods*, Wiley Interscience, New York, **1960**.
- [35] G. Psomas, C. Dendrinou-Samara, P. Philippakopoulos, V. Tangoulis, C. P. Raptoulou, E. Samaras, D. P. Kessissoglou, *Inorg. Chim. Acta* **1998**, *272*, 24.
- [36] I. Turel, *Coord. Chem. Rev.* **2002**, *23*, 27.
- [37] G. Palu, S. Valisena, G. Ciarocchi, B. Gatto, M. Palumbo, *Proc. Natl. Acad. Sci. USA* **1992**, *89*, 9671.
- [38] M. Lee, A. L. Rhodes, M. D. Wyatt, S. Forrow, J. A. Hartley, *Biochemistry* **1993**, *32*, 4237.
- [39] S. Arounaguir, B. G. Maiya, *Inorg. Chem.* **1996**, *35*, 4267.
- [40] H. Chao, W. J. Mei, Q. W. Huang, L. N. Ji, *J. Inorg. Biochem.* **2002**, *92*, 165.
- [41] T. M. Kelly, A. B. Tossi, D. J. McConnell, T. C. Strekas, *Nucleic Acids Res.* **1985**, *13*, 6017.
- [42] A. M. Pyle, J. P. Rehmman, R. Meshoyrer, C. V. Kumar, N. J. Turro, J. K. Barton, *J. Am. Chem. Soc.* **1989**, *111*, 3051.
- [43] E. K. Efthimiadou, M. Katsarou, Y. Sanakis, C. P. Raptoulou, A. Karaliota, N. Katsaros, G. Psomas, *J. Inorg. Biochem.* **2006**, *100*, 1378.
- [44] A. E. Friedman, J. C. Chambron, J. P. Sauvage, N. J. Turro, J. K. Barton, *J. Am. Chem. Soc.* **1990**, *112*, 4960.
- [45] I. Haq, P. Lincoln, D. Suh, B. Norden, B. Z. Chowdhry, J. B. Chaires, *J. Am. Chem. Soc.* **1995**, *117*, 4788.
- [46] Mudasir, K. Wijaya, N. Yoshioka, H. Inoue, *J. Inorg. Biochem.* **2003**, *94*, 263.
- [47] S. Satyanarayana, J. C. Dabrowiak, J. B. Chaires, *Biochemistry* **1992**, *31*, 9319.
- [48] B. Chaires, S. Satyanarayana, D. Suh, I. Fokt, T. Przewloka, W. Priebe, *Biochemistry* **1996**, *35*, 2047.
- [49] R. P. Hertzberg, P. B. Dervan, *J. Am. Chem. Soc.* **1982**, *104*, 313.
- [50] B. K. Santra, P. A. Reddy, G. Neelakanta, S. Mahadevan, M. Nethaji, A. R. Chakravarty, *J. Inorg. Biochem.* **2002**, *89*, 191.
- [51] T. Hirohama, Y. Karunuki, E. Ebina, T. Suzaki, H. Arai, M. Chikira, P. T. Selvi, M. Palaniandavar, *J. Inorg. Biochem.* **2005**, *99*, 1205.
- [52] A. Barve, A. Kumbhar, M. Bhat, B. Joshi, R. Butcher, U. Sonawane, R. Joshi, *Inorg. Chem.* **2009**, *48*, 9120.
- [53] U. Weser, L. M. Schubotz, E. Lengfelder, *J. Mol. Catal.* **1981**, *13*, 249.
- [54] J. Casanova, G. Alzuet, J. Borrás, J. Latorre, M. S. Sanau, S. García-Granda, *J. Inorg. Biochem.* **1995**, *60*, 219.
- [55] F. Cotton, G. Wilkinson, *Advanced Inorganic Chemistry*, Wiley, New York, **1972**.
- [56] J. A. Fee, *Metal Ions in Biological Systems* (Ed.: H. Siegel) Marcel Dekker, New York, Vol. 13, **1981**.
- [57] A. I. Vogel, *Textbook of Quantitative Inorganic Analysis*, 4th ed., ELBS and Longman, London, **1978**.
- [58] F. Neve, A. Crispini, S. Campagna, S. Serroni, *Inorg. Chem.* **1999**, *38*, 2250.
- [59] G. Cohen, H. Eisenberg, *Biopolymers* **1969**, *8*, 45.
- [60] M. E. Reichmann, S. A. Rice, C. A. Thomas, P. Doty, *J. Am. Chem. Soc.* **1954**, *76*, 3047.
- [61] A. Wolfe, G. H. Shimer, T. Meehan, *Biochemistry* **1987**, *26*, 6392.
- [62] T. Maniatis, E. F. Fritsch, J. Sambrook, *Molecular Cloning: A laboratory manual*; Cold Spring Harbor Laboratory Press, New York, **1989**.
- [63] A. M. Ramadan, M. M. El-Naggar, *J. Inorg. Biochem.* **1996**, *63*, 143.

Received: July 09, 2011

Published Online: November 29, 2011